

CHARACTERIZATION AND ANALYSIS OF PEROVSKITE OXIDE $\text{Sr}_2\text{FeCoO}_6$ SYNTHESIZED BY GEL-COMBUSTION PROCESS

*S. K. DURRANI, N. HUSSAIN, K. SAEED, M. AHMAD¹, M. SIDDIQUE¹ N. AHMAD and N. K. QAZI

Materials Division, Directorate of Technology, PINSTECH, P.O. Nilore, Islamabad, Pakistan

¹Physics Division, Directorate of Science, PINSTECH, P.O. Nilore, Islamabad, Pakistan

(Received December 18, 2009 and accepted in revised form February 26, 2010)

The microscopic and well-dispersed strontium iron cobalt based ($\text{SrFe}_{0.5}\text{Co}_{0.5}\text{O}_3$) perovskite oxide powders have been synthesized by nitrate-citrate gel-combustion process with stoichiometric composition variation of metal nitrate salts and citric acid. Crystallinity and phase analysis were performed by X-ray diffraction (XRD). Inspection of XRD patterns revealed that almost pure single phase $\text{SrFe}_{0.5}\text{Co}_{0.5}\text{O}_3$ cubic Pm3m symmetry was obtained. Morphology of sintered specimens was examined by scanning electron microscopy (SEM). It was observed that grain size of sintered samples increases with calcination temperature. XRD and SEM observations revealed that the crystal formation and morphology of $\text{SrFe}_{0.5}\text{Co}_{0.5}\text{O}_3$ oxide were dependent on the precursors and pH of precursor solutions. Thermal decomposition of gel precursor was investigated by thermogravimetric analysis (TG/DTA). ^{57}Fe Mössbauer spectroscopic studies on as-synthesized and calcined specimens have confirmed the uniform dispersion of Fe^{3+} ions in the tetrahedral framework of $\text{SrFe}_{0.5}\text{Co}_{0.5}\text{O}_3$.

Keywords: Citrate-nitrate gel combustion, Strontium iron cobalt oxide, Perovskite oxide, FTIR, Mössbauer analysis

1. Introduction

The perovskite-type oxides have the general formula ABO_3 , in which A represents a large electropositive cation and B represents a small transition metal ion. The perovskite structure can be described as a framework of corner-shared BO_6 octahedra which contain A cations at 12-coordinate sites. Double perovskite-type oxides have the formula $\text{A}_2\text{B}'\text{B}''\text{O}_6$, in which the primes indicate the different ions in different oxidation states, and the cations at the B sites, B' and B'', are regularly ordered, i.e., 1:1 arrangement of B' and B'' ions has been observed over the six-coordinate B sites. Since the B cations generally determine the physical properties of perovskites, different kinds of B' and B'' ion should show a variety of the physical properties of double perovskite oxides [1]. Perovskite oxides system have gained immense importance because of their potential application in many areas such as in high temperature solid state electrochemical fuel cells, electrodes, electro-catalysis and sensors [2-3]. These materials also hold great promise as ceramic membranes used to separate oxygen from

air because they are impervious to other gases [4-5]. The $\text{A}_2\text{BB}'\text{O}_6$ materials are especially interesting in view of the possibility that B and B' cations could be ordered at the octahedral sites, giving rise to novel electrical and magnetic properties due to B-O-B' [6]. Several novel perovskites have been prepared by grinding and calcination of oxides and carbonates [7]. This method involves high temperatures and thus sinters the final product, resulting in nonuniformity of particle size and shape, high impurity content and loss of fine particle nature. The electrical and structural ceramic components require good homogeneity in composition and microstructure, high purity and high reliability. As regard with the synthesis of oxides wet-chemical methods have been extensively recognized as an efficient approach to prepare these oxides at low temperatures. The most common and widely used wet chemical methods for the preparation of nanoscale transition metal oxides are co-precipitation [8] sol-gel [9], micro-emulsion [10], solvothermal and hydrothermal [11]. These processes have many advantages and disadvantages depending on desired properties

*Corresponding author : durransk@gmail.com

and applications. Recently, a simple and versatile gel-combustion synthesis has emerged as an important technique for synthesis and processing of advanced ceramics (structural and functional), catalysts, composites, alloys and nanomaterials [12]. In gel-combustion synthesis, the exothermicity of the redox (reduction-oxidation or electron transfer) chemical reaction is used to produce useful materials. Gel-combustion is an attractive method for the manufactures of technologically useful materials at low costs compared to conventional ceramic process. This technique has many advantages such as homogeneous mixing, good stoichiometric control, and the production of active submicron-size particles in a relatively short processing time [13-14]. The present work was carried out to study the preparation of strontium iron cobalt based crystalline perovskite-type oxide ($\text{Sr}_2\text{FeCoO}_6$) by citrate-nitrate gel-combustion process in order to observe the change in physicochemical characteristics of synthesized oxide product on the basis of X-ray diffraction, SEM, TG/DTA, FTIR and Mössbauer spectroscopic analysis.

2. Experimental

2.1. Materials and synthesis

Analytical reagent grade chemicals were used without further purification, metal nitrate salts, citric acid and sodium hydroxide from Fluka.

Strontium iron cobalt based oxide (2:1:1 ratio) powders were synthesized using citrate-nitrate gel-combustion process. Known concentration of nitrate solutions were prepared by dissolving different metal nitrates i.e., strontium, iron and cobalt nitrates in carbonate free (CO_3^{2-}) double deionized water (DDW). These solutions were then mixed and appropriate amount of citric acid was finally added in the mixed solution. Ammonium hydroxide was added drop wise and pH of suspension was maintained at 6.2 (acidic nature) with attached pH-meter (J. P. Selecta 2006, Spain). The dark brown mixture was evaporated at 70°C in rotary evaporator (Heidolph Laborota 4001) maintained at $70\text{-}80^\circ\text{C}$ for 4h. As a result, the viscosity raised due to the crosslinking of carboxylato-metal complexes into a three dimensional structure with ionic metal carboxyl and ammonium-carboxyl bonds or hydrogen bond, and on further dehydration a viscous sol was obtained. The viscous sol was transferred into a bowl and

was heated on a hot plate at $\sim 250^\circ\text{C}$. The gel was submitted to a sudden raising of the temperature up to $250\text{-}300^\circ\text{C}$, that brought about the boiling and swelling of the gel with evolution of a large amount of nontoxic gases (CO_2 , H_2O , N_2). The flameless combustion started in the hottest zones of the bowl and propagated from the bottom to the top like the eruption of a volcano. A rapid and auto-combustion reaction was completed within a few minutes as shown in Figure 1(a, b) giving dark



Figure 1 (a-b). Gel-combustion process for strontium iron cobalt based ($\text{SrFe}_{0.5}\text{Co}_{0.5}\text{O}_3$) perovskite oxide powder. (a) Combustion at 250°C (b) Black brown powder collected after combustion.

black-brown voluminous powder that fill almost completely the bowl. Alternatively, in order to better control the ignition temperature and

standardize the preparation procedure, the dried gel was put in a preheated oven at 300 °C instead of a hot plate. The resultant powder was calcined at different temperatures for various durations. Powder compacts were pressed using uni-axil hydraulic press of load capacity 25ton/in² (1ton/in² = 15.444 MPa) and sintered to dense at 1100 - 1200 °C for 4h with heating and cooling rates of 2 °C/min.

2.2. Characterization

The crystallinity and phase analysis were conducted by X-ray diffraction using Rigaku Geiger flux instrument with CuK_α radiation ($\lambda = 0.154056$ nm). The XRD data were collected in the 2θ range from 15°<2 θ <80° by step-scanning 0.05° increments and scanning rate of 5°/min. Microstructural features of synthesized materials and sintered pellets were observed by scanning electron microscope (LEO 440I). The samples for SEM observation were prepared by 10 min ultrasonic dispersion of a small amount of sample in ethanol and drop of the solution was put onto aluminum stud and dried in air and then coated via gold sputtering. The elemental composition of synthesized oxide materials were measured by electron probe micro analyzer (EPMA) attached with SEM. The unit cell content was calculated according to the procedure [15]. The organic and absorbed water molecules contents were measured by combined thermogravimetric (TG) and differential thermal analysis (DTA) using NETZSCH STA-409 simultaneous thermogravimetric analyzer. Samples were scanned from 30 to 900 °C in air at a flow rate of 200ml min⁻¹ and heating rate 10 °C min⁻¹. Fourier transform infrared (FTIR) spectra were measured using FTIR spectrometer Nicolet 6700, Thermo-Fisher, USA. The powders were dispersed in KBr and studied at room temperature. Mössbauer measurements were performed at room temperature using ⁵⁷Co source with the conventional constant acceleration-type Mössbauer spectrometer, calibrated with α -Fe foil. The data analysis has been performed using a computer programme MOS-90 [16] assuming that the peaks are Lorentzian.

3. Results and Discussion

Figure 2 shows the TG-DTA thermograms of as-synthesized SrFe_{0.5}Co_{0.5}O₃ oxide powder derived from precursor solution with pH 6.2. The

decomposition reaction is strongly endothermic which is evident from DTA plot. This decomposition is a single step combustion reaction as observed for different other compounds using TG / DTA

technique [17-18]. The endothermic peak at 125°C is attributed to the dehydration of trapped water and decomposition of partial alkaline solution in dried powder. The endothermic peak at 341°C is due to the decomposition of organic compounds i.e., citric acid, due to the conversion of aconitic acid C₆H₆O₆ (-H₂O) and itaconic acid C₅H₆O₄ (-CO₂), and an exothermic peak at about 452 °C associated with the complete decomposition of the polymerized itaconic acid [19]. Above 400-700 °C there is almost no weight loss. However, the corresponding DTA curve shows an endothermic peak at ~749 °C and there is no existence of other peaks between 760 and 900 °C. This indicates that there is no significant crystallization prior to that at ~750 °C. The endothermic peak at 749 °C showed the decomposition of residual carbonates, organics and their respective combining nitrates together with crystallization and phase formation of complex oxide SrFe_{0.5}Co_{0.5}O₃. Endothermic and exothermic peaks were found with an overall total weight loss of 37.05%. The position of minimum on DTA curve is basically determined by chemical composition of separated phase or by its transformation temperature.

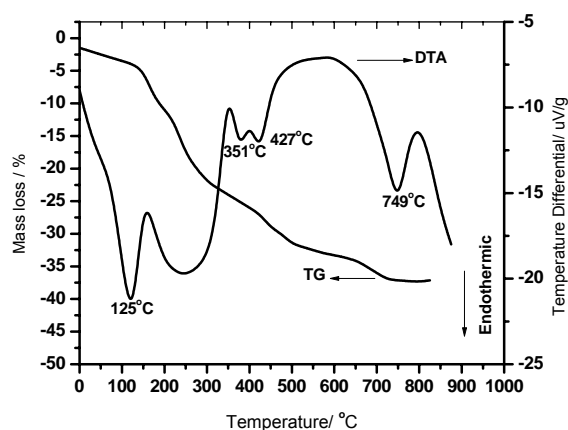


Figure 2. Thermal analysis TG/DTA of as-synthesized SrFe_{0.5}Co_{0.5}O₃ oxide powder.

Figure 3 shows the FTIR spectrum of dried (250°C) gel powder of strontium iron cobalt based oxide (SrFe_{0.5}Co_{0.5}O₃) synthesized by citrate-nitrate gel-combustion process. The observed

absorption bands and their respective assignments are presented in Table 1. The citrate-nitrate dried gel powder is a mixture of metal nitrates and citric acid.

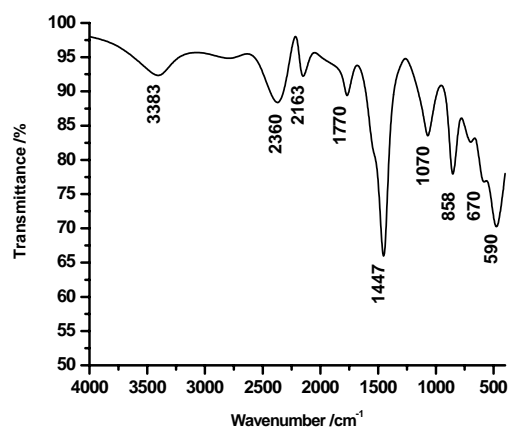


Figure 3. FTIR spectrum of dried (250 °C) gel powder of strontium iron cobalt based oxide ($\text{SrFe}_{0.5}\text{Co}_{0.5}\text{O}_3$) synthesized by citrate-nitrate gel-combustion process.

Table 1. FTIR analysis of $\text{SrFe}_{0.5}\text{Co}_{0.5}\text{O}_3$.

Wave numbers (cm^{-1})	Band assignment	Vibration mode
3383	$\nu\text{H}_2\text{O}$, $\nu\text{O-H}$ and $\nu\text{C-H}$	Asymmetric stretching
2360	$\nu\text{C-N}$	Asymmetric stretching
2160	$\nu\text{C=N}$	Symmetric stretching
1770	$\nu\text{C=O}$, $\nu\text{C=N}$	Stretching
1447	$\nu\text{C=O}$	Scissor and symmetric stretching
1070	$\nu\text{C-C}$, $\nu\text{C=N}$, $\nu\text{C=O}$	Stretching
858	$\nu\text{C-OH}$	Bending
670	$\nu\text{Co-O}$ $\nu\text{Fe-O}$, $\nu\text{Sr-O}$,	Bending
590	$\nu\text{Co-O}$ $\nu\text{Fe-O}$, $\nu\text{Sr-O}$,	Bending

The mixture consists of carboxyl group, a tetrahedral carbon, hydroxyl oxygen and metal oxygen. The absorption at 3383, 2360, 2160 cm^{-1} are due to νOH stretching mode, water and C-H stretch. The band at 1770, 1447 cm^{-1} are attributed to the $\nu\text{C=O}$ stretch [20]. The peak at 1070 cm^{-1} is due to $\nu\text{C-O}$ stretching. The FTIR characteristics peaks between 858, 670 and 590 cm^{-1} are stretching vibrations band in tetrahedral sites of metal-oxygen such as νCoO , νFeO and $\nu\text{Sr-O}$ and also due to $\nu\text{C-C}$ stretch. FTIR spectrum signifies the formation of $\text{SrFe}_{0.5}\text{Co}_{0.5}\text{O}_3$ crystalline phase. The result is confirmed by XRD phases as shown in Fig. 4.

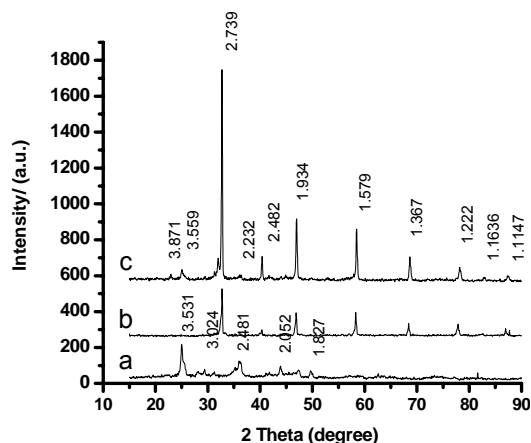
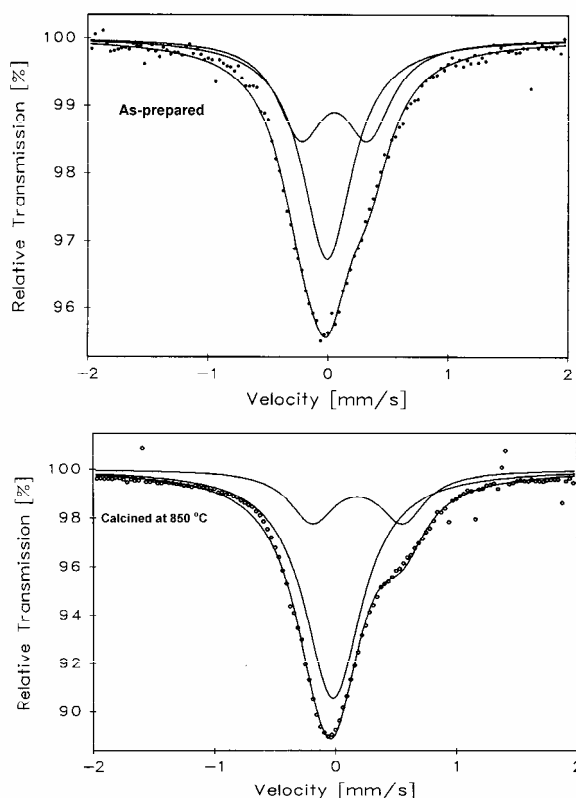


Figure 4. X-ray diffract pattern of $\text{SrFe}_{0.5}\text{Co}_{0.5}\text{O}_3$ oxide powder. a = synthesized oxide powder at 250 °C b = calcined oxide at 500 °C c = Calcined oxide at 850 °C

The XRD analysis was employed to determine the crystalline structure and phase purity of $\text{SrFe}_{0.5}\text{Co}_{0.5}\text{O}_3$ oxide. Figure 4(a-c) illustrates the XRD patterns of powders derived from the precursor solution with pH 6.2 and calcined at 250, 500 and 850 °C. The Fig. 3a shows XRD pattern of dried gel of citrate-nitrate after heating at 250 °C in air. The pattern indicates the sharp peaks of mixed metal nitrates and carbonates of cooked gel mixture. The most prominent SrCO_3 peaks were observed and indexed. Fig. 4b indicates the phases of $\text{SrFe}_{0.5}\text{Co}_{0.5}\text{O}_3$ oxide and tiny amount of carbonates after calcination at 500 °C. The single crystalline perovskite phase $\text{SrFe}_{0.5}\text{Co}_{0.5}\text{O}_3$ oxide was observed (Fig. 3c), when the sample was calcined at 850 °C. All relatively sharp peaks (Fig. 3c) were indexed and analysis was performed to obtain the lattice parameters and unit cell volume using ITO refinement programme software [21]. The analysis revealed that the calcined product is a good crystalline single phase cubic perovskite structure $\text{SrFe}_{0.5}\text{Co}_{0.5}\text{O}_3$ with space group Pm3m. The lattice cell parameters and unit cell volume values are 3.847(2) Å and 56.9333 Å³ respectively. The crystallographic XRD indexing results are presented in Table 2. These values were further confirmed by comparison with reported values JCPDS card No.46-0335 [22]. The unit cell parameters were found close to the reported values. There are no diffraction trace peaks of SrFe_2O_4 and SrCo_2O_4 in XRD pattern. The good agreement was observed between the refined crystallographic results and the Mössbauer spectra results shown in Figure 5.

Table 2. XRD indexing of SrFe_{0.5}Co_{0.5}O₃

d-spacing		Miller index		
Synthesized product	JCPDS #46-0335	h	k	l
3.871	3.858	1	0	0
2.739	2.728	1	1	0
2.239	2.227	1	1	1
1.934	1.929	2	0	0
1.579	1.574	2	1	1
1.367	1.366	2	2	0
1.222	1.219	3	1	0
1.163	1.163	3	1	1
1.114	1.113	2	2	2
System	Cubic			
Symmetry	Pm3m			
Unit cell parameter	3.847Å ^o			
Unit cell volume	56.933(Å ^o) ³			
Unit cell formula	Sr _{2.07} Fe _{1.08} Co _{1.12} O ₆ SrFe _{0.54} Co _{0.56} O ₃			

Figure 5. Mössbauer spectra of as-prepared and calcined samples of SrFe_{0.5}Co_{0.5}O₃.

Mössbauer spectra recorded at room temperature of as-synthesized and calcined samples are shown in Figure 5. Both spectra are asymmetrical paramagnetic singlet (single-line spectrum) like structure showing more than one type of Fe environments. Therefore, these are fitted with two subspectra (components), a quadrupole doublet (two-line spectrum) and a singlet indicating the paramagnetic nature of the material. The two paramagnetic components represent the two different cation environments. The quadrupole doublet originating from the electric field gradient of the surrounding environment shows the deviation of the system from the cubic symmetry. In perfect cubic symmetry arrangement of the oxygen ions in FeO₆ octahedra is regular and value of quadrupole splitting (Δ) should be nearly zero. The quadrupole doublet having $\Delta=0.56$ mm/s and isomer shift, $\delta=0.16$ mm/s is due to the Fe³⁺ at octahedral site and singlet (i.e. $\Delta=0.00$ mm/s) is due to Fe²⁺ at tetrahedral site, having cubic symmetry. It seems that Fe has mix type of ionic state in this material. When the specimen is heat-treated at 850 °C both Mössbauer parameters increased with temperature [23].

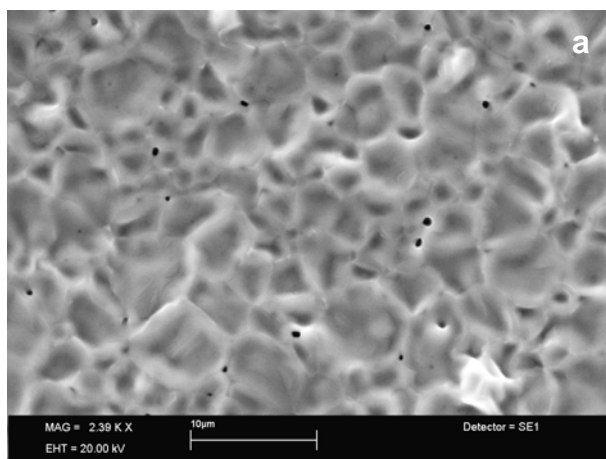
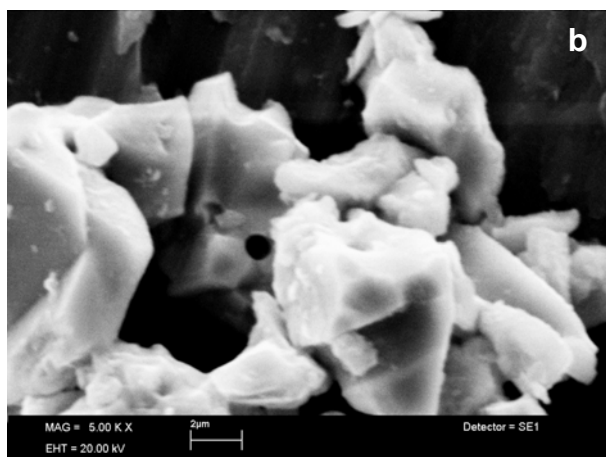


Figure 6. Morphology of SrFe_{0.5}Co_{0.5}O₃ perovskite-type oxide (a) sintered at 1100 °C (b) pellet sintered at 1200°C.

Figure 6 (a-b) shows SEM image of powder specimen SrFe_{0.5}Co_{0.5}O₃ oxide sintered at 1100 °C for 4h and pellet specimen sintered at 1200 °C for

2h respectively. It is shown that fine grains were grown in regular particle shape and agglomerated in narrow size distribution. The Fig.6a revealed that the powder specimen sintered at 1100°C for 4h has an average grain size of only about 2 µm (Fig.6a) whereas a much higher grain size of 10 µm resulted from pellet specimen sintered at 1200°C for 2h (Fig. 6b). The black spots in SEM micrographs are the pores.

Figure 7 shows the composition analysis of specimen sintered at 1200°C estimated by electron probe micro analyzer (EPMA). The unit cell formula was estimated using oxide formula method [15] and the results are given in Table 3. The result revealed that specimen consists of single perovskite phase with atomic ratio of strontium, iron and cobalt close to 2:1:1:6. Thus, the Sr_{2.07}Fe_{1.08}Co_{1.12}O₆ or Sr Fe_{0.54}Co_{0.56} O₃ oxide powder with nearly single perovskite phase was obtained.

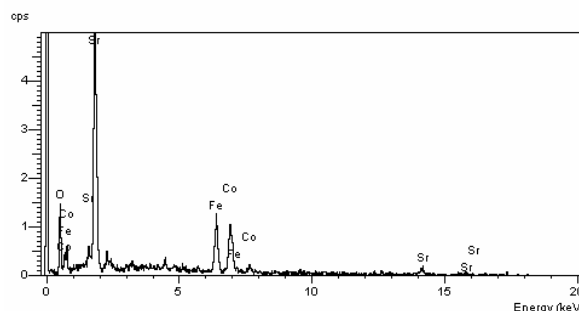


Figure 7. Composition analysis of EPMA curves of as synthesized SrFe_{0.5}Co_{0.5}O₃ oxide powder sintered at 1200 °C.

Table 3: Measurement of number of atoms per unit cell.

Elements	Composition		Mole ratios	No. of atoms per unit cell	
	Atomic %	Oxides %			
Strontium (Sr)	39.85	47.13	0.49	1.04	2.07
Fermium (Fe)	13.33	19.06	0.12	0.54	1.08
Cobalt (Co)	7.25	9.22	0.12	0.56	1.12
Oxygen [*]				2.99	5.99

*Calculated from empirical formula [15]

4. Conclusion

The fine and homogeneous crystals of $\text{SrFe}_{0.5}\text{Co}_{0.5}\text{O}_3$ perovskite oxide powder were grown by citrate- nitrate gel-combustion process. The grown crystals were characterized by FTIR spectroscopic, thermal studies, XRD and SEM. FTIR spectrum of crystals grown at 350 °C revealed the presence of O-H, C-O and Sr-O, Fe-O and Co-O bonds. The presence of compact water molecule was detected. The XRD and SEM studies confirmed that the citrate-nitrate gel-combustion process produces single phase perovskite $\text{SrFe}_{0.5}\text{Co}_{0.5}\text{O}_3$ powder. The synthesized product had composition uniformity, lower residual carbonates, nearly single perovskite phase with a ratio of strontium, iron and cobalt close to 2:1:1:6 ($\text{Sr}_{2.07}\text{Fe}_{1.08}\text{Co}_{1.12}\text{O}_6$ or $\text{SrFe}_{0.54}\text{Co}_{0.56}\text{O}_3$) and smaller particle size. Single perovskite phase $\text{SrFe}_{0.5}\text{Co}_{0.5}\text{O}_3$ powder, grain size (10 μm) was obtained from the pellet specimen sintered at 1200°C for 2h. Mössbauer spectroscopic studies on as-synthesized and calcined specimens have confirmed the uniform dispersion of Fe^{3+} ions in the tetrahedral framework of $\text{SrFe}_{0.5}\text{Co}_{0.5}\text{O}_3$.

Acknowledgements

Authors wish to thank Dr. Nasir Khalid, M. Ashaf Hussain and M. Arif for FITIR, XRD and thermal analysis respectively.

References

- [1] Y. Sasaki, Y. Doi and Y. Hinatsu, *J. Mater. Chem.* **12** (2002) 2361.
- [2] M.T. Anderson, K. B. Greenwood, G.A. Taylor and K.R. Poeppelmeier, *Prog. Solid State Chem.* **22** (1993) 197.
- [3] A. Maignan, C. Martin, N. Nguyen and B. Raveau, *Solid State Sci.* **3** (2001) 57.
- [4] Y. Teraoka H. M. Zhang, K. Okamoto, N. Yamazoe, *Mater. Res. Bull.* **23** (1988) 51.
- [5] B. Ma, U. Balachandran and J. H. Park, *Solid State Ionics* **83** (1996) 65.
- [6] J. B. Goodenough and J. M. Longo, in: K. Il. Hellwege (Ed.), *Landolt-Börnstein Tabellen, New Series III 4a*, Springer- Verlag, Berlin, (1970).
- [7] P. Hagenmuller, *Proc. Indian. Acad. Sci. (Chem. Sci)* **92** (1983) 1.
- [8] D. W. Johnson, Jr., in "Advances in Ceramics: Ceramic Powder Science; Vol. 21 American Ceramic Society (1987).
- [9] L. P. Zhou, J. Xu, X.Q. Li and F. Wang, *Mater. Chem. Phys.* **97** (2006) 137.
- [10] L. V. Hampden and M.J. Smith, *Chemistry of Advanced Materials: An Overview*; Wiley VCH: New York, (1998).
- [11] P. He, X. Shen and H. Gao, *J. Colloid Interface Sci.* **284** (2005) 510.
- [12] C. H. Lu and H. C. Wang, *J. Eur. Ceram. Soc.* **24** (2004) 717.
- [13] A. Varma, A. S. Rogachev, A.S. Mukasyan and S. Hwang, *Adv. Chem. Eng.* **24** (1998) 79.
- [14] R. Q. Chu and Z.J. Xu, *J. Electroceram.* **21** (2008) 778.
- [15] J. S. Thompson, *J. Chem. Edu.* **65** (1988) 704.
- [16] G. Große, *MOS-90 Version 2.2 Manual and Program Document Second Edition March* (1992).
- [17] S. K. Durrani, A.H. Qureshi, S. Qayyum and M. Arif. *J. Therm. Anal. Calorimetry* **95** (2009) 87.
- [18] S. K. Durrani, J. Akhtar, M. A. Hussain, A. H. Qureshi, M. Arif and M. Ahmad, *Mater. Chem. Phys.* **100** (2006) 324.
- [19] Y.M. Hon, K. Z. Fung and M. H.Hon, *J. Eur. Ceram. Soc.* **24** (2001) 515.
- [20] K. Suryanarayana, B.N. Das, H. B. Gon and K. V. Rao, *J. Mat. Sci. Lett.* **12** (1993) 1210.
- [21] J. W. Visser, *J. Appl. Crystallogr.* **2** (1969) 89.
- [22] JCPDS No. 46-0335, International Centre for Diffraction Data (2002).
- [23] K. Nomura, K. Tokumistu, T. Hayakawa and Z. Homonnay, *J. Radioanal. Nucl. Chem.* **246** (2000) 69.